Different Degrees of Disorder in Long Disordered Peptides Can Be Discriminated By Vibrational Spectroscopy.

ARTICLE *in* THE JOURNAL OF PHYSICAL CHEMISTRY B · APRIL 2013

Impact Factor: 3.3 · DOI: 10.1021/jp402869k · Source: PubMed

1 AUTHOR:

Reinhard Schweitzer-Stenner
Drexel University
219 PUBLICATIONS **4,370** CITATIONS

THE JOURNAL OF PHYSICAL CHEMISTRY B

Article

pubs.acs.org/JPCB

Different Degrees of Disorder in Long Disordered Peptides Can Be Discriminated by Vibrational Spectroscopy

Reinhard Schweitzer-Stenner*

Department of Chemistry, Drexel University, 3141 Chestnut Street, Philadelphia, Pennsylvania 19104, United States

ABSTRACT: The isotropic Raman, anisotropic Raman, IR, and vibrational circular dichroism (VCD) amide I profiles of a 20 residue homopeptide were calculated for different conformational mixtures that one would generally characterize as random coil or disordered. We first show that (1) pure polyproline II (pPII) coils, (2) statistical coils with different fractions pPII, β-strand, and right-handed helical residue conformations, and (3) ideal random coils (nearly equal probabilities for pPII, β, and right-handed helical) can be discriminated based on their respective VCD signal and, to a more limited extent, by means of the peak positions and asymmetries of the corresponding IR and Raman bands. Since molecular dynamics (MD) simulations of unfolded peptides (e.g., Aβ-segments) suggest a mixture of statistical coil and temporarily folded conformations, we calculated the amide I profiles of such mixtures composed of helical, β-strand, and disordered conformers and show that they give rise to rather distinct amide I profiles. Mixtures of regular structures with statistical coil segments can be discriminated from pure statistical and random coils by the amplitude of the negative amide I couplet in the VCD spectrum. We finally demonstrate the usefulness of such simulations by applying them to monomeric state of salmon calcitonin and the amyloid β fragment Aβ_{1-28}, for which NMR data provide evidence for a coexistence between statistical coil and helical conformations. Altogether, our results show that the combined use of the four amide I profiles provides spectroscopists with a powerful tool to discriminate between different conformational manifolds that long unfolded and disordered peptides and proteins might adopt in solution.

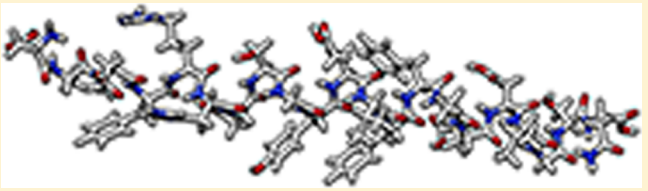

INTRODUCTION

It has been well established for over 50 years that the amide I mode of polypeptides gives rise to spectral bands in the respective IR and Raman spectra whose wavenumber positions are very sensitive indicators of secondary structures.[1] More recently, the vibrational circular dichroism (VCD) signal of this mode has been added to this arsenal of spectroscopic techniques.[2,3] This structural sensitivity is, to a major extent, due to vibrational mixing between local amide modes of individual peptide units, which link the amino acid residues in a polypeptide chain.[4−9] Individual amide I modes can be ascribed to a mixture of local vibrations dominated by the CO stretching modes of the peptide units.[10] Traditionally, amide I bands of IR spectra, and, to a lesser extent, of Raman spectra, are decomposed into symmetric bands assignable to different types of secondary structure, namely, right-handed α-helix, β-sheet, (unspecified) turns, and random coils.[11,12] While vibrational spectroscopy has thus become an indispensable tool for protein (and peptide) structure analysis, it is nevertheless considered a low-resolution technique incapable of providing site specific information even for very short peptides. However, recent advancements have led to a correction of this picture. Femtosecond time-resolved IR spectroscopy allows the determination of (average) amino acid conformations of polypeptides owing to its capability to extract orientational dependent excitonic coupling constants and relative orientations of transition dipole moments of coupled amide I modes.[13−18] Moreover, this technique emerged as a tool for exploring the dynamics of peptide (protein)−solvent interactions and its influence on amide IR band profiles.[19,20] A more conventional approach developed by our group combines IR, isotropic Raman, anisotropic Raman and VCD with J-coupling data from NMR to eventually obtain conformational distributions of individual amino acid residues in peptides of short and intermediate length.[21−25] In this context we have shown that by using these complementary vibrational techniques to measure amide I bands, one is able to discriminate between many types of secondary structures (i.e., different types of helices, turns, β-strands, and polyproline II (pPII) conformations), which makes it possible to identify and quantify different subpopulations of what is still incorrectly termed the "random coil state".[21,22,26,27]

The question arises of whether the discriminatory power of the combined amide I profiles can still be at least partially maintained for longer peptides (i.e., more than 10 residues) and eventually even proteins without resorting to very expensive site directed isotopic labeling. In this paper, we address this question by carrying out simulations of IR, Raman, and VCD amide I band profiles for various structural compositions of a 20mer peptide. Besides calculating the spectra of classical statistical coil mixtures, we also consider mixtures of statistical coil sections and temporarily formed secondary structures such as right-handed helices and hairpins. This is particularly important because intrinsically disordered peptides (IDPs) such as Aβ-peptide

Received: March 23, 2013
Revised: April 26, 2013
Published: April 30, 2013

fragments have been predicted to locally and temporarily form secondary structures.[28−30] We unambiguously show that particularly VCD is a very powerful tool for discriminating between different disordered conformations of a peptide.

THEORY

We have developed a model for simulating amide I profiles of IR, isotropic Raman and anisotropic Raman, and VCD spectra based on the classical excitonic coupling model described in numerous papers published over the last 10 years.[31−33] Here, we briefly focus solely on the basic principles. The validity of the excitonic coupling model for amide I modes, which considers vibrational coupling between excited vibrational states of individual oscillators, is based on the assumption that interacting amide I modes are clearly distinct with respect to their normal mode composition. That this is indeed the case has been nicely demonstrated by Cho and co-workers.[34,35] The interaction Hamiltonian of the system can be written as

$$\hat{H} = \sum_{j=1}^{N} \hat{H}_j^0 + \sum_{j=1}^{N-1} \hat{H}_{j,j+1} + \sum_{j=1}^{N-2} \sum_{k=j+2}^{N} \hat{H}_{j,k} \tag{1}$$

where $\hat{H}_j^0$ is the Hamiltonian of the unperturbed jth local oscillator, and $\hat{H}_{j,j+1}$ denotes the combined contribution of through-bond and through-space nearest neighbor coupling. N is the total number of residues in the considered polypeptide. For the latter, we recently developed a heuristic algorithm,[36] which invoked a combination of simple trigonometric relations to reproduce the contour map of coupling constants obtained by Torii and Tasumi.[9] Non-nearest coupling $\hat{H}_{j,k}$ is modeled in terms of the transition dipole coupling approach. Transition dipole moments and Raman tensors of excitonic states that can be expressed as linear combinations of transition dipole moments and Raman tensors of local oscillators. The coefficients of these expressions were obtained from diagonalizing the Hamiltonian in eq 1 in the basis set of local oscillators. In order to combine the transition dipole moments and Raman tensors of the local oscillators, they have to be transformed into a common coordinate system, which we positioned at the C-terminal residue.[31] This transformation and the conformational dependences of nearest neighbor and non-nearest neighbor coupling parameters bring about a backbone dependence of IR, Raman, and VCD profiles of amide I.

It should be noted that the VCD profiles of most conformational ensembles discussed in this paper were calculated with a formalism that neglects intrinsic rotational strengths of local amide I modes. Thus, we consider VCD as solely being induced by excitonic coupling between adjacent oscillators. In such a case, the integrated intensities of the entire signal (i.e., all positive and negative bands) is zero. Only for the simulation of the amide I′ VCD of the amyloid fragment Aβ_{1-28} were we forced to introduce intrinsic magnetic transition dipole moments of amide I′ oscillators in order to account for the asymmetric profile displayed in the experimental spectrum.

Our approach is by far more simplistic than recent band profile calculations based on time-dependent quantum mechanical descriptions of peptide−solvent systems or density functional theory (DFT)-based ab initio calculations,[19,20,37] but as shown several times, the empirical parametrization of our algorithm allows for a quantitative reproduction of experimental amide I band profiles.[21−23,26,27,38−40]

Our work on tripeptides has revealed the coexistence of various secondary structures in statistical coil distributions of individual amino acid residues. The ensemble is dominated by a subdistribution located in the region between canonical β-strand and pPII structures. Contrary to what was obtained for other residues, the pPII conformation is not strongly populated. Instead, more than 20% of the aspartic residues sample space in the upper right quadrant of the Ramachandran. The respective conformations are assignable to so-called type II asx-turns. Although somewhat nontraditional, these turns appear in proteins at ample occasions[41] and are stabilized by side-chain−backbone hydrogen bonding. In addition, we could discriminate a minor contribution to the conformational ensemble, which is reminiscent of conformations found at the i+2 positions of type II β-turns.[22,27]

For our analysis of tripeptides, we described such subensembles by two-dimensional Gaussian functions. This is not a feasible option for a 20mer peptide, because the sampling of a rather large number of microstates is computationally too costly. Instead, we follow the strategy first proposed by Schweitzer-Stenner and Measey[24] in that we describe considered subensembles of secondary structures by introducing representative conformations with average dihedral angels associated with the maxima of corresponding Gaussian functions. As later demonstrated by Verbaro et al.,[38] additional conformations associated with the half-width positions of the pPII distribution along the coordinates φ and ψ have to be considered. This is necessary because nearest-neighbor excitonic coupling, which dominates the interaction Hamiltonian for extended conformations, is extremely structure sensitive in the pPII region.[36] Altogether, we considered the representative structures listed in Table 1. To visualize these distributions, we created Ramachandran plots in which all conformations are represented by two-dimensional Gaussian distributions with half-widths of 20° (Figure 1). IR, Raman and VCD intensity profiles of the entire statistical ensemble were calculated as

$$I(\tilde{\nu}) = \sum_{k_1=1}^{m_1} \sum_{k_2=1}^{m_2} \cdots \sum_{k_N}^{m_N} \left(\sum_{i=1}^{N} I_{i,k_1\ldots k_N}(\tilde{\nu}) \prod_{j=1}^{N} \chi_{j,k_j} \right) \tag{2}$$

where the first N-sums run over all conformers of the residues 1, 2, 3, ..., N, m_j (j = 1, ..., N) denotes the number of conformers adopted by the jth-residue, $I_{i,k_1\ldots k_N}$ is the intensity associated with the transition into the ith excitonic state of a peptide conformation with the residues 1, 2, ..., N in conformations k_1, k_2, ..., k_N, respectively. The corresponding mole fractions of these conformations are denoted as χ_{j,k_j} and can be written as

$$\chi_{j,k_j} = \frac{e^{-G_{k_j}/RT}}{\sum_{k_j=1}^{m_j} e^{-G_{k_j}/RT}} \tag{3}$$

where G_{k_j} is the Gibbs energy of the kth conformation of the jth residue. As listed in Table 1, the conformations 1−5 are all located in the pPII region. Since the conformations 2−5 are associated with the half-width of the Gaussian pPII distribution along φ and ψ, the mole fractions χ_{j,k_j}, ..., χ_{j,k_j} are related to the total pPII fraction by

$$\chi_{j,k_2} = \chi_{j,k_3} = \chi_{j,k_4} = \chi_{j,k5} = \frac{1}{2}\chi_{j,k_1} \tag{4}$$

with

$$\chi_{j,k_{\mathrm{pPII}}} = \sum_{k=1}^{5} \chi_{j,k_j} \tag{5}$$

dx.doi.org/10.1021/jp402869k | J. Phys. Chem. B 2013, 117, 6927−6936

Table 1. Conformational Distributions Used to Simulate IR, Isotropic Raman, Anisotropic Raman and VCD Amide I Profile of a 20mer[a]

	φ,ψ[o]	pPII	sc1	sc2	rc
pPII	−70.0 150	0.32	0.2	0.08	0.06
pPII	−70.0 160	0.17	0.1	0.04	0.03
pPII	−70.0 140.0	0.17	0.1	0.04	0.03
pPII	−60.0 150.0	0.17	0.1	0.04	0.03
pPII	−80.0 150.0	0.17	0.1	0.04	0.03
βt	−115.0 160.0		0.15	0.155	0.175
βp	−115.0 134.0		0.1	0.155	0.175
βa	−140.0 125.0			0.215	0.175
IIβi+2	−60.0 0.0		0.1	0.2	0.1
rhα	−48.0 −57.0		0.05	0.035	0.195
L1	−67.0 20.0				
L2	−78.0 53.0				
L3	−64.0 39.0				
L4	−75.0 23.0				
L5	−28.0 0.0				

[a]Details are described in the text (sc1: statistical coil model 1; sc2: statistical coil model 2; rc: random coil model).

as the total pPII fraction. The intrinsic intensity profiles $I_{i,k_1...,k_N}(\tilde{\nu})$ of transitions into excitonic states can well be approximated by Gaussian functions.

In order to calculate the intensities $I_{i,k_1...,k_N}(\tilde{\nu})$ we considered nearest-neighbor through-bond coupling and non-nearest neighbor transition dipole coupling as previously described.[36] For the sake of simplicity, we assume that the intrinsic wavenumbers are identical for all nonterminal oscillators that sample conformations in the upper left-hand quadrant of the Ramachandran plot, in accordance with earlier reported experimental data. Results from DFT calculations suggest a downshift of wavenumbers for conformations in the region of right handed helical structures.[20] We used a shift of −15 cm^{-1} for recent analyses of amide I′ profiles of tripeptides.[26] From the same data we deduced a 5 cm^{-1} upshift for turn-like conformations located in the upper right quadrant of the Ramachandran plot (asx-turns and different β-turns).[27] We prefer such empirical adjustment over results from electrostatic calculations of peptide−water interactions, which have thus far not achieved a quantitative agreement with experimental data.

This paper reports the result of simulations for different conformational mixtures of a polypeptide with 20 amino acids. In the following, two types of mixtures are considered. Type I mixtures contains peptides with different sequences of conformations adopted by individual residues. The corresponding peptide conformations resemble either statistical or random coils. Type II mixtures encompass statistical coil/random coil ensembles and peptides with local secondary structures like helices, turns and β-sheets. The system is sufficiently long for mimicking the spectral properties of larger unfolded peptides and proteins, since its length exceeds the coherence length of excitonic states of amide I.[42] Since we considered up to 10 different conformations per amino acid residue (including the 5 pPII conformations introduced above), a complete statistical sampling of up to 10^{20} different peptide conformations rendered impossible. We therefore carried out a Monte Carlo like sampling of the conformational space by averaging the amide I profiles of 3000−4000 simulations for which the respective sequence of residue conformations were selected from the considered set of representative structures by a stochastic algorithm in our Matlab program. This strategy can be illustrated by the following example. Consider a pentapeptide with five residues. Let us assume that each residue can solely adopt pPII, a β-strand and a right handed helical conformation. We assign the numbers 1, 2, and 3 to these residue conformations. The program randomly selects sequences such as 1,2,1,3,1, calculates the respective amide I profiles, and weighs it with a statistical factor given by the product of the mole fractions of the considered residue conformations (c.f. eq 2). This process is repeated several times for different, stochastically selected sequences. The final amide I profiles are then calculated as the average over these simulations. Convergence is checked by comparing the averaging for different numbers of simulations.

RESULT AND DISCUSSION

Randomization of Local and Excitonic Energies. All amide I oscillators are subject to inhomogeneous broadening.[13,14,20,43,44] This is particularly the case if they are fully

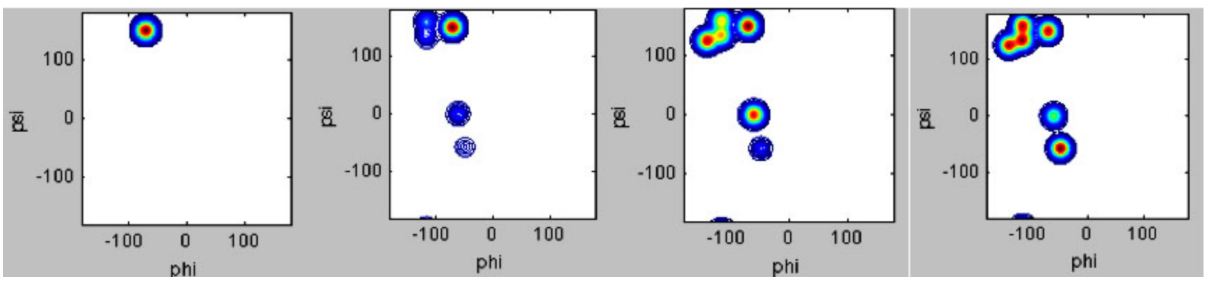

Figure 1. Illustrative Ramachandran plots of distributions used to simulate amide I profiles of a disordered 20mer peptide. From left to right: pPII only, sc1, sc2, and rc. The coordinates of the troughs are listed in Table 1. Each trough was modeled as a two-dimensional distribution with a total half-width of 20°. In our simulation, we represented most of these subdistributions with a representative structure. Only pPII was represented by five values for reasons given in the text.

dx.doi.org/10.1021/jp402869k | J. Phys. Chem. B 2013, 117, 6927−6936

hydrated and thus subject to hydrogen bonding with water. While experiments in D_2O eliminate vibrational mixing between amide I and water bending modes, fluctuations of the hydrogen network can still induce wavenumber fluctuations over a very broad time scale.[19,20] In most of our studies we dealt with this issue in a rather simplistic way by just assuming Gaussian distributions of excitonic energies.[45] We showed recently for the two amide I oscillators of tripeptides that uncorrelated broadening effects, which bring about distributions of differences between the eigenenergies of local oscillators and thus distributions of excitonic mixing between excited vibrational states,[19,20] would produce rather sharp band structures.[46] Their absence in the respective experimentally obtained amide I band profiles led us to conclude that uncorrelated fluctuations of solvent molecules do not provide a significant contribution to widths of these profiles. However, while this might be true for nearest-neighbors in tripeptides, the situation could be different in longer polypeptides where the differences between (unperturbed) local eigenenergies are small and non-nearest neighbor coupling contributes to the excitonic Hamiltonian.[32,45,47,48] In order to understand the possible influence of uncorrelated broadening effects on the amide I profiles of poypeptides, we started our series of simulations by calculating the amide I band profiles of what we term the "statistical coil distribution I" (Table 1, Figure 1) with different mixtures of excitonic and intrinsic broadening. The solid lines in Figure 2 exhibits the amide I profiles calculated for a broadening of 5 cm^{-1} (half half-width) for each excitonic transition. This corresponds to the natural homogeneous half-width of amide I bands of trialanine in D_2O.[13] In principle, we should have used Lorentzian profiles for this particular case, but we stuck to Gaussian profiles for all simulations, since this is the more appropriate choice if transitions are inhomogeneously broadened. Generally, the differences do not matter for the purposes of this study. IR and Raman profiles resulting from our calculations are asymmetric with shoulders on both sides, which are most pronounced in the isotropic Raman spectrum. They certainly result from the wavenumber shifts assumed for helical and turn like conformations. The negative VCD-couplet is rather strong and symmetric. Next, we considered an intrinsic inhomogeneous Gaussian broadening of 10 cm^{-1} (half half-width) of local transition energies combined with an excitonic broadening of 5 cm^{-1}. This led to the dash−dash profiles in Figure 2. As expected, the broadening of local transition energies broadens the profiles and decreases their asymmetry. The VCD-couplet appears quite deformed with the negative maximum downshifted below 1640 cm^{-1}. Finally, we considered broadening a 11 cm^{-1} solely on the level of the excitonic transitions. This value, which corresponds to the effective half-width of the second simulation ($\approx(10^2 + 5^2)^{1/2}$ cm^{-1}), is close to half-widths used for a satisfactory reproduction of experimental band profiles of tri- and tetrapeptides.[49,50] The dash−dot line in Figure 2 shows the result of this calculation. Apparently, the IR and Raman band profiles are very similar to those obtained with the second calculations. This indicates that for longer peptides, IR and Raman profiles alone can hardly be used to discriminate between inhomogeneities on the local oscillator or excitonic state level. This is not the case for the VCD couplet, for which the pure excitonic broadening model produced a symmetric shape, which is closer positioned to the IR band as the profile obtained from the second simulation. As we will show at the end of the paper, this is what one generally obtains experimentally. Therefore, we will stick to

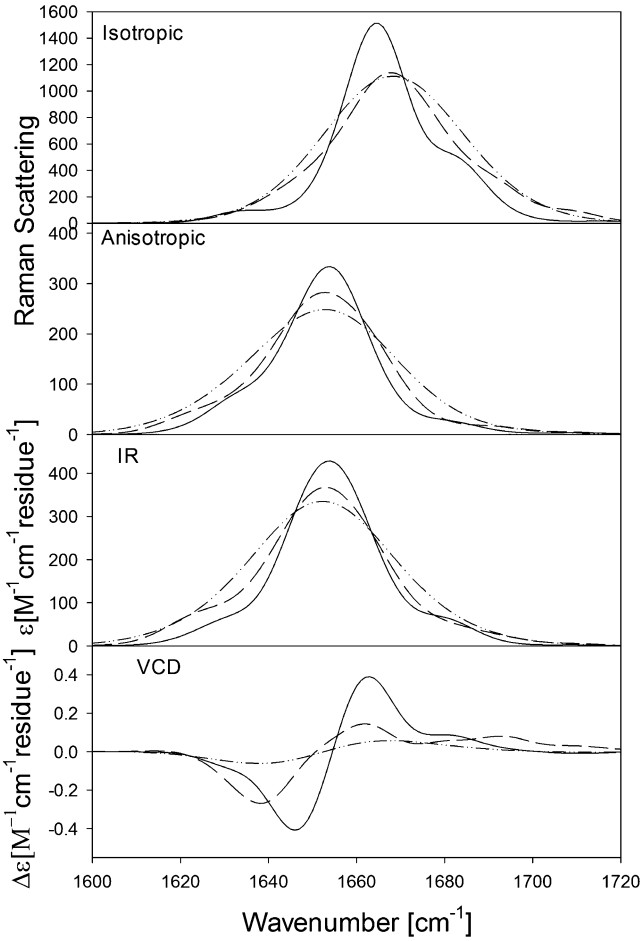

Figure 2. Simulated IR, isotropic Raman, anisotropic Raman, and VCD amide I profiles of an unblocked 20mer peptide for homogeneously broadened excitonic transition (half half-width 6 cm^{-1}) (solid line), homogeneous broadening of 6 cm^{-1} combined with inhomogeneous broadening described as a convolution of stochastic variations of wavenumbers of local modes (±9 cm^{-1}) and additional broadening (±9 cm^{-1}) of excitonic transitions (dashed line). The total broadening per excitonic transition for this scenario is 12.3 cm^{-1} and a total 12 cm^{-1} broadening of each excitonic transition. The simulations were performed for the statistical coil formation described in the text.

the excitonic broadening model, i.e., assuming moderate stochastic variations of the local eigenenergies and much of the broadening to occur on the excitonic level.

Extended and Coil Conformations. In this section we consider profiles of different type I mixtures and compare them with a hypothetical homogeneous peptide with all residues in pPII (Figure 1). Figure 3 shows the isotropic Raman, anisotropic Raman, IR and VCD band profiles of the amide I modes of a 20-residue peptide for the conformational ensembles listed in Table 1. The solid line was calculated for a pPII helix. The pPII distributions was centered at $\varphi = -70°$, $\psi = 150°$ with a half half-width of 10° in φ and ψ direction. This is a rather realistic model for a poly-L-proline peptide if all residues are in their *trans*-conformation (we did not consider the redshift of intrinsic amide I frequencies for proline residues, though), but it is not a realistic model even for polyalanine peptides. Even if one assumes a pPII mole fraction of 0.9 per residue (this value has been inferred from NMR data of trialanine by Graf et al.[51]), the probability of finding all residues in pPII would be only 0.12. However, this is an overestimation

dx.doi.org/10.1021/jp402869k | J. Phys. Chem. B 2013, 117, 6927−6936

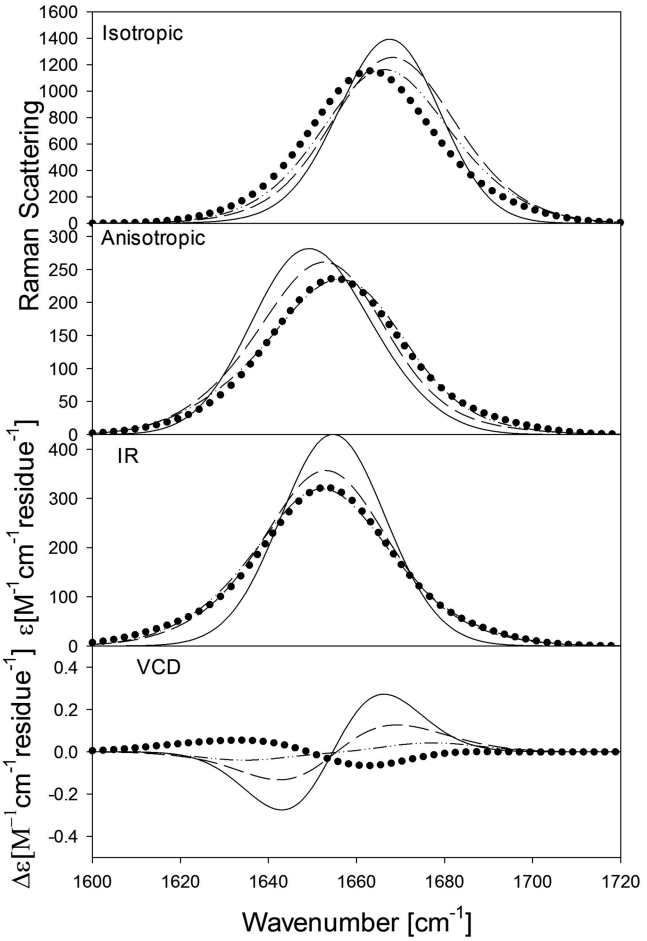

Figure 3. Simulated IR, isotropic Raman, anisotropic Raman, and VCD amide I profiles of an unblocked 20mer peptide for all residues adopting a pPII conformation (solid line), statistical coil mode I (dashed line), statistical coil model II (dash−dot line), and random coil (dot−dot line).

since the pPII propensity of alanine is lower than 0.9 in longer polyalanines since nearest-neighbor interaction stabilize right-handed helical conformations.[38,51,52] Here we use the result for an all-pPII peptide solely as a standard to which the spectral band profiles of more heterogeneous ensembles can be compared. In quantitative agreement with experimental results for poly-L-proline, the VCD exhibits a pronounced negative couplet with an amplitude of ± 0.25 $M^{-1}cm^{-1}residue^{-1}$.[53] The IR-band position is substantially red-shifted with respect to the peak of isotropic Raman scattering, a common feature of extended pPII and β-strand structures.[45] The splitting between these bands is a measure of the nearest-neighbor excitonic coupling strength. The anisotropic Raman bands is positioned closer to the IR band. All bands are only moderately asymmetric.

The dashed lines in Figure 3 visualize the amide I profiles of statistical coil mixture 1 (Figure 1), which is still predominantly pPII, but contains substantial contributions from β-strand, turn-like, and right-handed helical conformations. Extended conformations (pPII and β-strand) together are still dominant. This is a rather realistic approach for many though not all nonalanine amino acid residues.[21,26,54] The increased heterogeneity leads to a broadening of the IR profile, which also becomes slightly more asymmetric toward lower energies. The Raman profiles broaden only slightly, but a redshift of the anisotropic Raman profile is noteworthy. The amplitude of the VCD-couplet is substantially reduced to $\sim \pm 0.11$ M^{-1} cm^{-1} $residue^{-1}$, which again demonstrates the earlier reported structural sensitivity of this band.[21,22,36] Next, we simulated the amide I profile of another statistical coil distribution, "statistical coil distribution 2" (Table 1, Figure 1), which has higher and more equally distributed β-strand content and a lesser pPII content. In the trough of right-handed helical structures, the distribution is shifted toward type II β_{i+2} conformations, in line with coil library distributions of many amino acid residues.[26,55] The corresponding IR profiles of statistical coil I and II are nearly indistinguishable, whereas the isotropic and anisotropic Raman profiles of coil II appear slightly red- and blue-shifted with respect to the coil I band. The VCD couplet of coil II appears further reduced compared with that of coil I, the amplitude is now at 0.04 M^{-1} cm^{-1} $residue^{-1}$. Finally, we simulated the amide I profiles of an ideal random coil composition in which occupations are evenly distributed over pPII, all β-strand conformation, type II β_{i+2}, and right-hand α-helical regions of the Ramachandran plot (Table 1, Figure 1). IR and anisotropic Raman profiles of this random coil and the above introduced statistical coil structure are practically identical, whereas the isotropic band of the former appears even more red-shifted. The VCD is again qualitatively different in that it now shows a weak positive couplet. Taken together, the results of this first set of simulations indicate that IR and Raman profiles of statistical and random coils are very similar but broader than the profile of a pure pPII distribution. It is noteworthy that the isotropic and anisotropic Raman band red- and blueshifts with increasing conformational disorder, thus reducing the respective non-coincidence with the IR-band position. The VCD band is the most structurally sensitive of all four amide I bands. Random and statistical coil have a much weaker signal than, e.g., a pure pPII distribution and give rise to differentiable type of signals. This makes the absolute amplitude $\Delta\varepsilon_{max}$ or the Kuhn anisotropy $\Delta A_{max}/A_{max}$ (A: absorptivity) of amide I an important experimental indicator of conformational disorder.

Mixtures of Coils and Regular Secondary Structures. In this section we describe the simulation for type II mixtures. These simulations are motivated by results from molecular dynamics (MD) simulations, which suggest that even disordered peptides such as Aβ can locally and temporarily adopt secondary structures such as helices, turns, and even β-sheets.[28−30,56] In a first step, we calculate the amide I profiles of common secondary structure components ($\alpha\alpha$, $\alpha\beta$,$\beta\beta$, etc) connected by loops, turns or coil conformations. Subsequently, the amide I profiles of type II mixtures of coiled peptides and partially structured peptides are calculated. Figure 4 compares the amide I profiles of the following secondary structures: (a) two six-residue helical segments connected by a coil I section of six residues and two coil I end groups, (b) two antiparallel oriented helices formed by six and seven residues, respectively, connected by a 5-residue loop structure, (c) a hairpin structure with two antiparallel β-strands formed by six and seven residues, respectively, connected by a type I β-turn, (d) a β-strand (six residues)-coil I-β-strand (six residues) conformation, and (e) a helix (6 residues)-coil I-β-strand (6 residues) conformation. The dihedral angles of the loop and turn structures are listed in Table 2. Statistical coil I conformations were assumed for the two terminal residues. For comparison, the amide I profile of statistical coil II is plotted again as a representative of the considered set of disordered ensembles. The most regular structures (b and c) are shown in Figure 5. As depicted

dx.doi.org/10.1021/jp402869k | J. Phys. Chem. B 2013, 117, 6927−6936

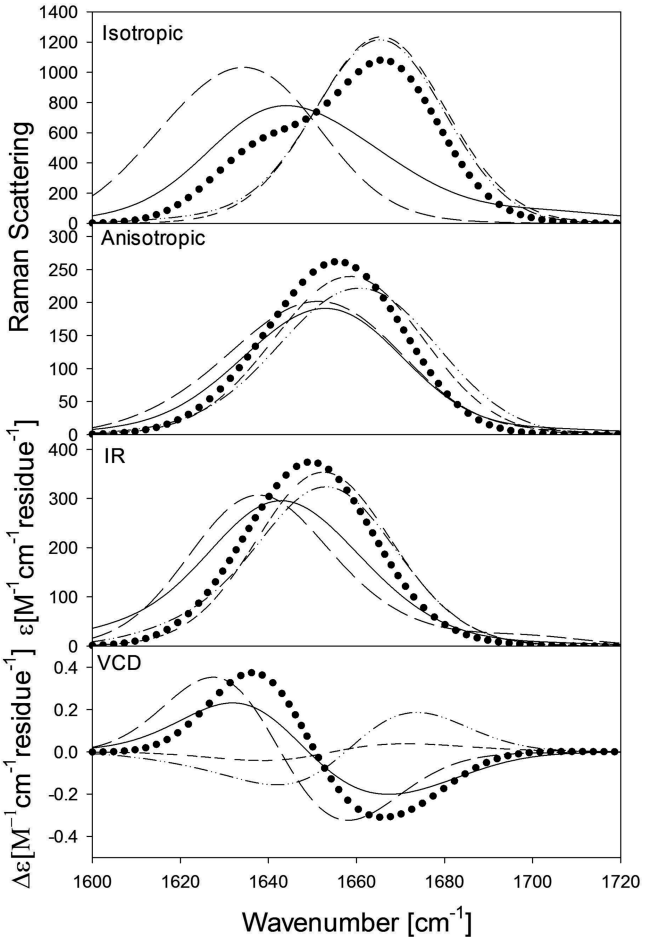

Figure 4. Simulated IR, isotropic Raman, anisotropic Raman, and VCD amide I profiles of an unblocked 20mer peptide for helix−coil−helix (solid line), double helix (long dash), β-hairpin (dash−dot−dot), aβ−coil−aβ (short dash), and helix−coil−aβ (dot−dot).

Table 2. Dihedral Coordinates in Degree of Turns Used for Double-Helix (Loop DH) and Hairpin Conformations

	ϕ,ψ[o] loop hairpin	ϕ,ψ[o] loop double-helix
L1	−113.91	−67.0
	168.61	20.0
L2	−56.5	−78.0
	22.11	53.0
L3	−119.53	−64.0
	14.32	39.0
L4	−151.42	−75.0
	121.61	23.0
L5	−113.21	−28.0
	173.16	0.0

in Figure 4, the profiles of these mixtures of secondary structures are clearly different. This particularly holds for isotropic Raman and VCD. As one expects due to the different local wavenumbers for the respective structures, the isotropic Raman profiles of β-strand containing mixtures are substantially blue-shifted compared with those of predominantly helical peptides. The isotropic Raman profiles of β-strand and helical structures are asymmetric toward the high- and low-wavenumber region, respectively. Corresponding differences of anisotropic Raman and IR profiles are less pronounced, but still significant, particularly for the IR profile, which appears at lower wavenumbers in the β-strand spectrum. With

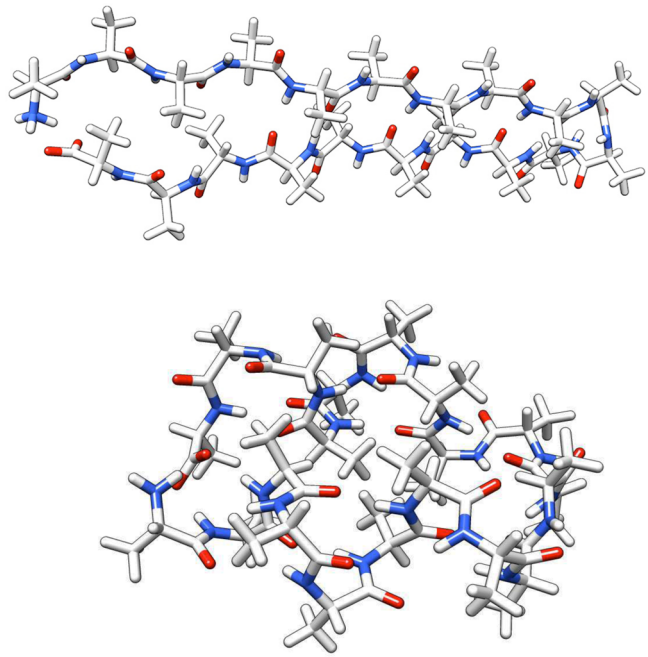

Figure 5. Structural representation of a 20mer polyalanine in a β-hairpin (upper figure) and a double helix (lower figure) structure. The dihedral angles chosen for creating these structures have also been used in the simulations described in the text.

regard to VCD, all helix containing structures (a,b, and e) exhibit positive couplets. The antiparallel double helix (b) shows a somewhat weaker and slightly blueshifted signal compared with the VCD of a helix−coil-I−helix conformation (a). Interestingly, the VCD of helix−coil−helix and helix−coil−strand are rather similar, owing to the weak contribution of the β-strand segment.[48,57] The VCDs of conformations mostly containing β-strand motifs are all weak negative couplets. Taken together, our results show that isotropic Raman, VCD, and, to a lesser extent, IR are the best tools to discriminate between the secondary structures discussed in this paragraph.

We now calculated the amide I by averaging over a type II mixture of five statistical coil II peptides and five peptides adopting the conformations (a−e), respectively. This mixture could be representative of an IDP or protein that temporarily adopts different types of secondary structures. In Figure 6, the resulting band profiles are compared with those obtained for statistical coil II and an ideal random coil. The isotropic Raman band of the above type II mixture is broader than the corresponding profile of the pure random coil peptides and much less asymmetric than that of the statistical coil I. The respective IR and anisotropic Raman profiles, however, are only slightly different and would be difficult to distinguish experimentally. Again, VCD emerges as the most sensitive technique. The signal of the mixture is, by more than a factor 2, less intense than those of statistical coil I, and qualitatively different from the positive couplets of both statistical coil mixtures. It exhibits a weak W-shape. This is certainly due to the larger fraction of residues in right handed helical or β-strand conformations. Altogether, the spectra in Figure 5 indicates that isotropic Raman combined with VCD could be used to distinguish different mixtures of totally and partially disordered peptides and proteins from those without any secondary structure. With respect to VCD, all our results suggest that attention must be paid either

dx.doi.org/10.1021/jp402869k | J. Phys. Chem. B 2013, 117, 6927−6936

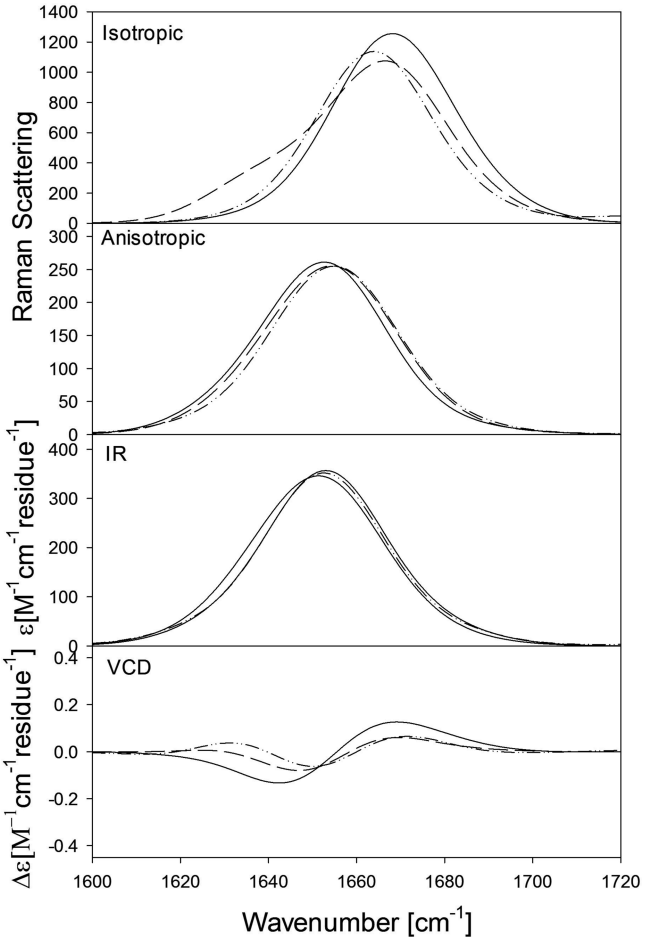

Figure 6. Comparison of amide IR, isotropic Raman, anisotropic Raman and VCD profiles of random coil (dash–dot–dot), statistical coil I (dashed line), and a mixture of 10% helix–coil–helix, 10% double helix, 10% hairpin, 10% aβ–coil–aβ, 10% helix–coil–aβ and 50% statistical coil I (solid line).

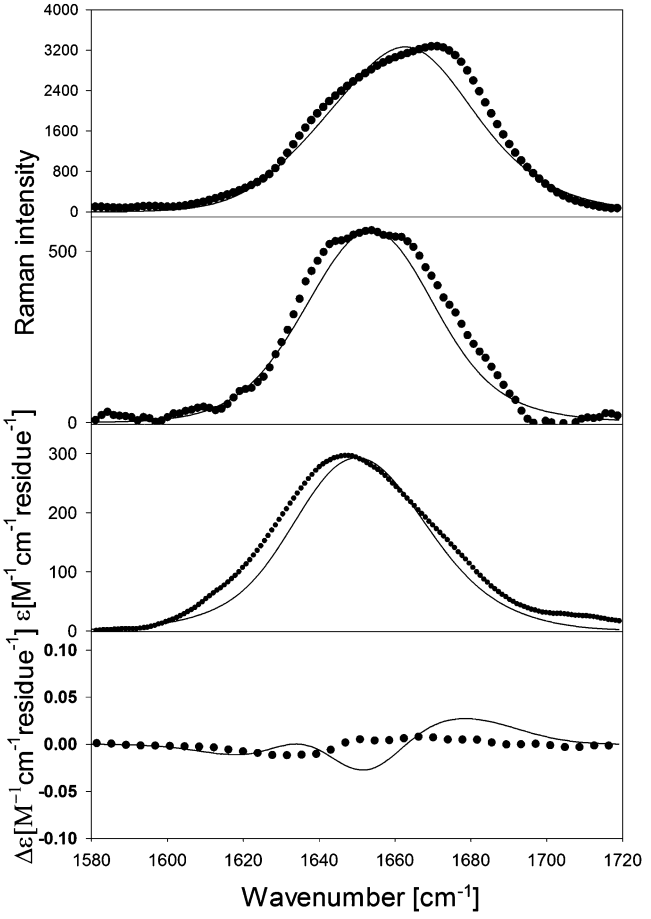

Figure 7. Amide I′ profiles of the isotropic Raman, anisotropic Raman, IR, and VCD of salmon calcitonin measured in D_2O at acidic pH (2.0). The data were first reported by Schweitzer-Stenner et al.[58] The solid lines result from a simulation described in the text.

to the absolute intensity of the signal or its anisotropy, if one wants to use it for characterizing disordered states.

Comparison with Experimental Data. In this context, a qualitative comparison with earlier experimental data from our group is useful. In what follows, we compare two sets of experimental amide I profiles of IDPs with simulated profiles for which we assumed different type II mixtures of coil and regular structures. The conformational mixtures used to closely resemble the experimental amide I profiles should be considered as representative average, since we do not make an attempt to consider differences between the conformational propensities of the amino acid residues of the peptide.[54] The same distribution function is rather assumed for all residues in the coil fraction of the peptide.

First, we analyzed the amide I′ IR, Raman, and VCD profiles of monomeric hormone salmon calcitonin in D_2O at acidic pD. These data have been reported earlier.[58] The peptide contains 32 amino acid residues. These profiles are shown in Figure 7. An inspection of the amide I' spectra of the two peptides reveals rather similar broad and asymmetric Raman and IR bands, which could be indicative of a statistical or random coil. The noncoincidence between IR and isotropic Raman indicates a dominance of extended conformations with residues sampling the upper left quadrant of the Ramachandran plot, which would be consistent with a statistical coil.[45] The VCD is practically nonexistent, also indicating either a random coil or a statistical coil with some admixture of sporadically formed helices. We simulated such a situation for our 20mer peptide. The solid line in Figure 7 was calculated as a type II mixture of 90% statistical coil II and 10% of the above introduced helix–coil–helix conformation. The total pPII fraction is 0.21. Since we do not consider regular secondary structures and do normalize our intensities on the number of residues, our 20mer is fully representative of 32 residues containing calcitonin.[42] As displayed in Figure 6, the simulations are very close to the experimental data. This is particularly true for the asymmetric IR and Raman profiles. The VCD is slightly overestimated. A fine-tuning might require an explicit consideration of propensities of individual amino acid residues,[21,22,26,27] which is beyond the scope of this paper. It should be noted that the literature data, including our own earlier analysis, suggest indeed that salmon calcitonin adopts a mixture of coil and unstable helical structures.[58]

In a second step we analyzed the amide I′ profiles of the amyloid beta fragment Aβ_{1-28} in acidic D_2O. The data were reported earlier by Eker et al.,[59] and interpreted as indicating a rather high pPII fraction in the secondary structure distribution of the peptide. This is indeed what the comparatively strong amide I′ VCD signal in Figure 7 suggests, which clearly distinguishes Aβ_{1-28} from calcitonin. The other amide I′ profiles (i.e., IR and Raman) are only slightly different, but those of salmon calcitonin are generally broader. All these data already reveal (a) that

dx.doi.org/10.1021/jp402869k | J. Phys. Chem. B 2013, 117, 6927–6936

conformational distributions of different IDPs are not necessarily identical (contrary to what the random coil model suggests) and that they can be distinguished by vibrational spectroscopy. The solid line in Figure 8 results from a simulation calculated as a type II

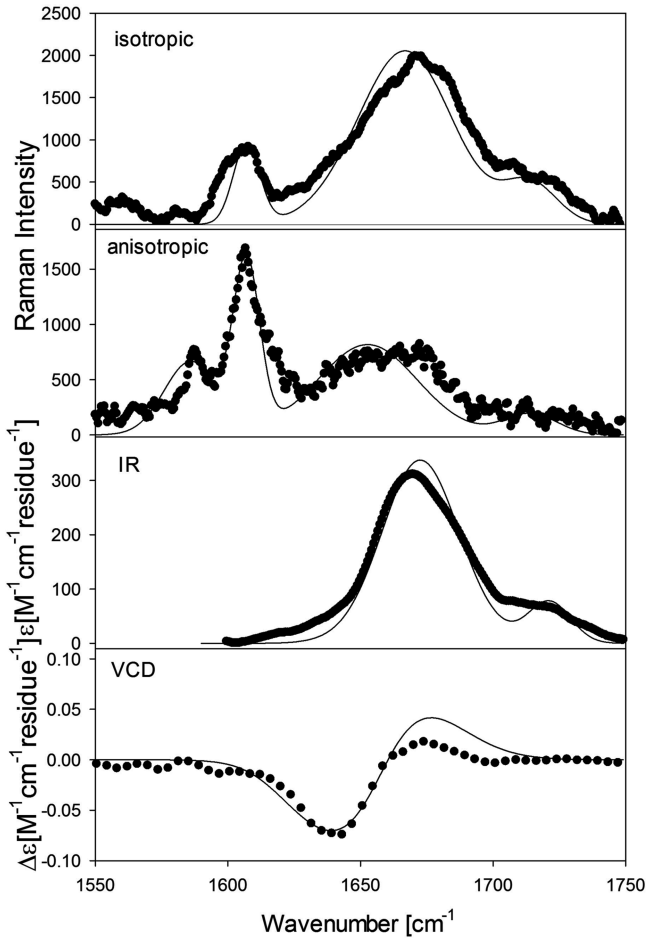

Figure 8. Amide I′ profiles of the isotropic Raman, anisotropic Raman, IR, and VCD of $A\beta_{1-28}$ measured in D_2O at acidic pH (2.0). The data were first reported by Eker et al.[59] The solid lines result from a simulation described in the text.

mixture of a slightly modified statistical coil I (95%) and 5% of the above introduced helix−coil−aβ conformation (the pPII fraction was slightly larger (0.66), and the total β-strand fraction slightly lower (0.3) than the statistical coil II values listed in Table 1). In order to account for the nonconservative VCD signal, we had to allow for some individual rotational strength of amide I oscillators by introducing a magnetic transition moment of 1.1×10^{-5} D. Any attempts to increase the fraction of regular structures would require an even higher pPII fraction to account for the measured VCD signal. The fraction of temporarily folded structures in the conformational ensemble of $A\beta_{1-28}$ is most likely small, contrary to what MD simulations suggest.[28] While these simulations cannot be regarded as an accurate conformational analysis of the two peptide, they clearly reveal a much larger total pPII fraction of in the conformational distribution of $A\beta_{1-28}$ (0.63 to be compared with 0.21 of salmon calcitonin).

CONCLUSION AND SUMMARY

It is still widely believed that vibrational spectroscopy is a low-resolution technique that would certainly unable to facilitate the exploration of disordered or unfolded peptides and proteins. Over the last 5 years we and others have shown that this notion is definitely untrue for short peptides, for which a combination of IR, Raman, VCD, and NMR coupling constants yielded quite detailed information about conformational distributions of individual amino acids. In addition, we have previously shown that, if applied to peptides of moderate length (7−11 residues), our techniques can be used to check the validity of different conformational models. This paper demonstrates that even for longer peptides, particularly, the amide I profile of VCD spectra can particularly serve as a tool to discriminate between different types of peptide disorder. Isotropic Raman and to a lesser extent IR can also become valuable tools. It is not possible to deduce residue specific conformational distributions directly from amide I profiles. However, if combined with NMR data (i.e., J coupling constants and NOE data) different models used to reproduce such NMR data can additionally be checked by simulating the respective amide I profile. The current study shows the discriminatory power of the amide I profile if embedded in such a comprehensive strategy is substantial. Our reanalysis of the amide I′ profiles of salmon calcitonin and $A\beta_{1-28}$ shows that quantitative estimate of structural differences between IDPs is even possible in the absence of additional NMR data. A clear disadvantage of the vibrational spectroscopic methods discussed in this paper and of NMR spectroscopy is the rather high sample concentration (20 mg/mL to obtain a good Raman signal) needed for these experiments, which restricts all these methods to peptides and proteins with high solubility in water and low propensities for self-aggregation.

AUTHOR INFORMATION

Corresponding Author

*Phone: 215-895-2268; fax: 215-895-1265; e-mail: rschweitzer-stenner@drexel.edu.

Notes

The authors declare no competing financial interest.

ACKNOWLEDGMENTS

The author thanks Siobhan E. Toal for a very critical reading of and very valuable comments on this manuscript.

REFERENCES

(1) Bandekar, J.; Krimm, S. Normal Mode Spectrum of the Parallel-Chain β-Sheet. *Biopolymers* **1988**, *27*, 909−921.

(2) Keiderling, T. A. Vibrational Circular Dichroism: Application to Conformational Analysis of Biomolecules. In *Circular Dichroism and the Conformational Analysis of Biomolecules*; Fasman, G. D., Ed.; Plenumn Press: New York, 1996; p 555.

(3) Keiderling, T. A.; Xu, Q. Unfolded Proteins Studied with IR and VCD Spectra. *Adv. Protein Chem.* **2002**, *62*, 111−161.

(4) Krimm, S.; Bandekar, J. Vibrational Spectroscopy of Peptides and Proteins. *Adv. Protein Chem.* **1986**, *38*, 181.

(5) Krimm, S.; Mark, J. E. Conformations of Polypeptides with Ionized Side Chains of Equal Length. *Proc. Natl. Acad. Sci. U.S.A.* **1968**, *60*, 1122−1129.

(6) Lee, S.-H.; Krimm, S. An Ab-Initio Based Vibrational Analysis of α-Poly(L-alanine). *Biopolymers* **1998**, *46*, 283−317.

(7) Torii, H.; Tasumi, M. Application of the Three-Dimensional Doorway-State Theory to Analyses of the Amide-I Band of Globular Proteins. *J. Chem. Phys.* **1992**, *97*, 92−98.

(8) Torii, H.; Tasumi, M. Model Calculations on the Amide-I Infrared Bands of Globular Proteins. *J. Chem. Phys.* **1992**, *96*, 3379−3387.

(9) Torii, H.; Tasumi, M. Ab Initio Molecular Orbital Study of the Amide I Vibrational Interactions Between the Peptide Groups in Di- and Tripeptides and Considerations on the Conformation of the Extended Helix. *J. Raman Spectrosc.* **1998**, *29*, 81−86.
(10) Mirkin, N. G.; Krimm, S. Ab Initio Vibrational Analysis of Hydrogen-Bonded *trans*- and *cis*-*N*-Methylacetamide. *J. Am. Chem. Soc.* **1991**, *113*, 9742−9747.
(11) Bandekar, J. Amide Modes and Protein Conformation. *Biochim. Biophys. Acta* **1992**, *1120*, 123−143.
(12) Surewicz, W. K.; Mantsch, H. H. New Insight into Protein Secondary Structure from Resolution-Enhanced Infrared Spectra. *Biochim. Biophys. Acta* **1988**, *952*, 115−130.
(13) Woutersen, S.; Hamm, P. Structure Determination of Trialanine in Water Using Polarized Sensitive Two-Dimensional Vibrational Spectroscopy. *J. Phys. Chem. B* **2000**, *104*, 11316−11320.
(14) Woutersen, S.; Hamm, P. Isotope-Edited Two-Dimensional Vibrational Spectroscopy of Trialanine in Aqueous Solution. *J. Chem. Phys.* **2001**, *114*, 2727−2737.
(15) Hamm, P.; Lim, M.; DeGrado, W. F.; Hochstrasser, R. Stimulated Photon Echos from Amide I Vibrations. *J. Phys. Chem. B* **1999**, *103*, 10049−10053.
(16) Kim, S.; Hochstrasser, R. M. The 2D IR Responses of Amide and Carbonyl Modes in Water Cannot Be Described By Gaussian Frequency Fluctuations. *J. Phys. Chem. B* **2007**, *111*, 9697−9701.
(17) Kim, Y. S.; Wang, J.; Hochstrasser, R. M. Two-Dimensional Infrared Spectroscopy of the Alanine Dipeptide in Aqueous Solution. *J. Phys. Chem. B* **2005**, *109*, 7511−7521.
(18) Paul, C.; Wang, J.; Wimley, W. C.; Hochstrasser, R. M.; Axelsen, P. Vibrational Coupling, Isotropic Editing, and β-Sheet Structure in a Membrane-Bound Polypeptide. *J. Am. Chem. Soc.* **2004**, *126*, 5843−5850.
(19) Gorbunov, R. D.; Kosov, D. S.; Stock, G. *Ab Initio*-Based Exciton Model of Amide I Vibrations in Peptides: Definition, Conformational Dependence and Transferrability. *J. Chem. Phys.* **2005**, *122*, 224904−224915.
(20) Gorbunov, R. D., Nguyen, P. H., Kobus, M. & Stock, G. (**2007**). Quantum-Classical Description of the Amide I Vibrational Spectrum of Trialanine. *J. Chem. Phys. 126*.
(21) Hagarman, A.; Measey, T. J.; Mathieu, D.; Schwalbe, H.; Schweitzer-Stenner, R. Intrinsic Propensities of Amino Acid Residues in GxG Peptides Inferred from Amide I Band Profiles and NMR Scalar Coupling Constants. *J. Am. Chem. Soc.* **2010**, *132*, 540.
(22) Hagarman, A.; Mathieu, D.; Toal, S.; Measey, T. J.; Schwalbe, H.; Schweitzer-Stenner, R. Amino Acids with Hydrogen-Bonding Side Chains Have an Intrinsic Propensity to Sample Various Turn Conformations in Aqueous Solution. *Chem.—Eur. J.* **2011**, *17*, 6789−6797.
(23) Pizanelli, S.; Forte, C.; Monti, S.; Zandomeneghi, G.; Hagarman, A.; Measey, T. J.; Schweitzer-Stenner, R. Conformation of Phenylalanine in the Tripeptides AFA and GFG Probed by Combining MD Simulations with NMR, FTIR, Polarized Raman and VCD Spectroscopy. *J. Phys. Chem. B* **2010**, *114*, 3965−3978.
(24) Schweitzer-Stenner, R.; Measey, T. The Alanine-Rich XAO Peptide Adopts a Heterogeneous Population, Including Turn-like and PPII Conformations. *Proc. Natl. Acad. Sci. U.S.A.* **2007**, *104*, 6649−6654.
(25) Schweitzer-Stenner, R.; Measey, T.; Hagarman, A.; Dragomir, I.The Structure of Unfolded Peptides and Proteins Explored by Vibrational Spectroscopy. In *Instrumental Analysis of Intrinsically Disordered Proteins: Assessing Structure and Conformation.*; Uversky, V. N., Longhi, S., Eds.; Wiley & Sons: Chichester, U.K., 2010; pp 171−224.
(26) Schweitzer-Stenner, R.; Hagarman, A.; Toal, S.; Mathieu, D.; Schwalbe, H. Disorder and Order in Unfolded Peptides and Proteins: A View Derived from Tripeptide Conformational Analysis. I. Tripeptides with Long and Predominantly Hydrophobic Side Chains. *Proteins* **2013**, *81*, 955−967.
(27) Rybka, K.; Toal, S.; Verbaro, D.; Mathieu, D.; Schwalbe, H. Disorder and Order in Unfolded Peptides and Proteins: A View Derived from Tripeptide Conformational Analysis. II. Tripeptides with Short Side Chains Populating Asx and β-Type Like Turn Conformations. *Proteins* **2013**, *81*, 968−983.
(28) Dong, X.; Chen, W.; Mousseau, N.; Derreumaux, P. Energy Landscape of the Monomer and Dimer of the Alzheimer's Peptide Aβ(1−28). *J. Chem. Phys.* **2008**, *128*, 125108.
(29) Barz, B.; Urbanc, B. Dimer Formation Enhances Structural Differences between Amyloid β-Protein (1−40) and (1−42): An Explicit-Solvent Molecular Dynamics Study. *PLoS One* **2012**, *7*, e34345.
(30) Wise-Scira, O.; Xu, L.-R.; Kitahara, T.; Perry, G.; Coskuner, O. Amyloid β Peptide Structure in Aqueous Solution Varies with Fragment Size. *J. Chem. Phys.* **2011**, *135*, 205101.
(31) Schweitzer-Stenner, R. Dihedral Angles of Tripeptides in Solution Determined by Polarized Raman and FTIR Spectroscopy. *Biophys. J.* **2002**, *83*, 523−332.
(32) Schweitzer-Stenner, R. Advances in Vibrational Spectroscopy As a Sensitive Probe of Peptide and Protein Structure. A Critical Review. *Vib. Spectrosc.* **2006**, *42*, 98−117.
(33) Schweitzer-Stenner, R. Conformational Analysis of Unfolded Peptides by Vibrational Spectroscopy. In *Unfolded Proteins: From Denatured States to Intrinsically Disordered*; Creamer, T. A., Ed.; Novalis Press: New York, 2008; pp 101−142.
(34) Choi, J.-H.; Ham, S.; Cho, M. Local Amide I Mode Frequencies and Coupling Constants in Polypeptides. *J. Phys. Chem. B* **2003**, *107*, 9132−9138.
(35) Choi, J.-H.; Kim, J.-S.; Cho, M. Amide I Vibrational Circular Dichroism of Polypeptides: Generalized Fragmentation Approximation Method. *J. Chem. Phys.* **2005**, *122*, 174903-1−174903−11.
(36) Schweitzer-Stenner, R. Distribution of Conformations Sampled by the Central Amino Acid Residue in Tripeptides Inferred From Amide I Band Profiles and NMR Scalar Coupling Constants. *J. Phys. Chem. B* **2009**, *113*, 2922−2932.
(37) Jansen, T. C.; Dijkstra, A.; Watson, T. M.; Hirst, J. D.; Knoester, J. Modelling of the Amide I Bands of Small Peptides. *J. Chem. Phys.* **2006**, *125*, 044132.
(38) Verbaro, D.; Ghosh, I.; Nau, W. M.; Schweitzer-Stenner, R. Discrepancies between Conformational Distributions of a Polyalanine Peptide in Solution Obtained from Molecular Dynamics Force Fields and Amide I′ Band Profiles. *J. Phys. Chem. B* **2010**, *114*, 17201−17208.
(39) Verbaro, D.; Mathieu, D.; Toal, S. E.; Schwalbe, H.; Schweitzer-Stenner, R. Inoized Trilysine: A Model System for Understanding the Nonrandom Structure of Poly-L-lysine and Lysine-Containing Motifs in Proteins. *J. Phys. Chem. B* **2012**, *116*, 8084−8094.
(40) Duitch, L.; Toal, S.; Measey, T. J.; Schweitzer-Stenner, R. Triaspartate: A Model System for Conformationally Flexible DDD Motifs in Proteins. *J. Phys. Chem. B* **2012**, *116*, 5160−5171.
(41) Duddy, W. J.; Nissink, J. M. M.; Allen, F. H.; Milner-White, E. J. Mimicry by Asx and ST-Turns of the Four Main Types of β-Turn in Proteins. *Protein Sci.* **2004**, *13*, 3051−3055.
(42) Hayashi, T.; Mukamel, S. Vibrational-Exciton Couplings for the Amide I, II, III and A Modes of Peptides. *J. Phys. Chem. B* **2007**, *111*, 11032−11046.
(43) Woutersen, S.; Pfister, R.; Hamm, P.; Mu, Y.; Kosov, D. S.; Stock, G. Peptide Conformational Heterogeneity Revealed from Nonlinear Vibrational Spectroscopy and Molecular-Dynamics Simulations. *J. Chem. Phys.* **2002**, *117*, 6833−6840.
(44) Measey, T.; Hagarman, A.; Eker, F.; Griebenow, K.; Schweitzer-Stenner, R. Side Chain Dependence of Intensity and Wavenumber Position of Amide I′ in IR and Visible Raman Spectra of XA and AX Dipeptides. *J. Phys. Chem. B* **2005**, *109*, 8195−8205.
(45) Schweitzer-Stenner, R. Secondary Structure Analysis of Polypeptides Based on an Excitonic Coupling Model to Describe the Band Profile of Amide I′ of IR, Raman, and Vibrational Circular Dichroism Spectra. *J. Phys. Chem. B* **2004**, *108*, 16965−16975.
(46) Toal, S. E.; Meral, D.; Verbaro, D. J.; Urbanc, B.; Schweitzer-Stenner, R. The pH-Independence of Trialanine and the Effects of Termini Blocking in Short Peptides: A Combined Vibrational, NMR,

UVCD, and Molecular Dynamics Study. *J. Phys. Chem. B* **2013**, *117*, 3689−3706.
(47) Huang, Q.; Schweitzer-Stenner, R. Conformational Analysis of Tetrapeptides by Exploiting the Excitonic Coupling between Amide I Modes. *J. Raman Spectrosc.* **2004**, *53*, 586−591.
(48) Schweitzer-Stenner, R. Simulated IR, Isotropic and Anisotropic Raman, and Vibrational Circular Dichroism Amide I Band Profiles of Stacked β-Sheets. *J. Phys. Chem. B* **2012**, *116*, 4141−4153.
(49) Eker, F.; Cao, X.; Nafie, L.; Schweitzer-Stenner, R. Tripeptides Adopt Stable Structures in Water. A Combined Polarized Visible Raman, FTIR and VCD Spectroscopy Study. *J. Am. Chem. Soc.* **2002**, *124*, 14330−14341.
(50) Schweitzer-Stenner, R.; Eker, F.; Griebenow, K.; Cao, X.; Nafie, L. The Conformation of Tetraalanine in Water Determined by Polarized Raman, FTIR and VCD Spectroscopy. *J. Am. Chem. Soc.* **2004**, *126*, 2768−2776.
(51) Graf, J.; Nguyen, P. H.; Stock, G.; Schwalbe, H. Structure and Dynamics of the Homologous Series of Alanine Peptides: A Joint Molecular Dynamics/NMR Study. *J. Am. Chem. Soc.* **2007**, *129*, 1179−1189.
(52) Gnanakaran, S.; Garcia, A. E. Validation of an All-Atom Protein Force Field: From Dipeptides to Larger Peptides. *J. Phys. Chem. B* **2003**, *107*, 12555−12557.
(53) Measey, T.; Schweitzer-Stenner, R. Simulation of Amide I′ Band Profiles of *trans* Polyproline Based on an Excitonic Coupling Model. *Chem. Phys. Lett.* **2005**, *408*, 123−127.
(54) Schweitzer-Stenner, R. Conformational Propensities and Residual Structures in Unfolded Peptides and Proteins. *Mol. BioSyst.* **2012**, *8*, 122−133.
(55) Sosnick, T. R. Sampling Library http://godzilla.uchicago.edu/cgi-bin/rama.cgi.
(56) Chong, S.-H.; Ham, S. Conformational Entropy of Intrinsically Disordered Protein. *J. Phys. Chem. B.* **2013**, *117*, 5503−5509.
(57) Bour, P.; Keiderling, T. A. Structure, Spectra and the Effects of Twisting of β-Sheet Peptides. A Density Functional Theory Study. *J. Mol. Struct. (THEOCHEM)* **2004**, *675*, 95−105.
(58) Schweitzer-Stenner, R.; Measey, T.; Hagarman, A.; Eker, F.; Griebenow, K. Salmon Calcitonin and Amyloid β: Two Peptides with Amyloidogenic Capacity Adopt Different Conformational Manifolds in Their Unfolded States. *Biochemistry* **2006**, *45*, 2810−2819.
(59) Eker, F.; Griebenow, K.; Schweitzer-Stenner, R. Aβ_{1-28} Fragment of the Amyloid Peptide Predominantly Adopts a Polyproline II Conformation in an Acidic Solution. *Biochemistry* **2004**, *43*, 6893−6898.